High altitude Project Tesla transmitter, Leadville, Colorado

A quarter-wave coaxial cavity as a power processing plant

Mark Nash, James Smith, Robert Craven
339 Engineering Sciences Building
West Virginia University
MORGANTOWN, West Virginia 26506
United States of America

The coaxial conductor geometry has been a subject of interest in electrical engineering since the advent of radio and the foundations of the radio engineering discipline. The simplicity of this geometry and the resonant modes associated with it, have attracted scientists to return to the development of different technologies and analytic models utilizing the coaxial geometry time and again. Almost all of these have been developed in the areas of communication technologies and have utilized portions of classical transmission line theory for the basis of their respective analytic models.

The limited scope of communication technologies has focused attention to a limited level (small energies) of applications of the complex electromagnetic nature of resonant circuits and physical properties they possess which may be exploited. The analytical simplicity of the coaxial geometry provides for a distributed resonant structure which has modes that can be physically interpreted and visualized with qualitative links to the analysis through transmission line theory but, as is often the case, the complexity of model analysis of cavity resonators hinders the physical interpretation of their properties.

The coaxial resonator may be viewed as a transitional geometry falling between transmission line and cavity resonators. With a proper analytic synthesis of the field theory, transmission line models, the lumped equivalent model, and cavity and waveguide analytic considerations, a broader and more complete understanding of all distributed resonant structures may be gained.

It becomes apparent with a review of analytic models, that appreciation for the potential offered by resonant cavities as RF power processing elements has remained undeveloped. This essentially new area (RF Power Processing) of Radio Frequency Engineering has potential.

Lumped Circuits

The lumped equivalent transmission line model is presented in many undergraduate electromagnetics texts and is considered one of the classical analytic techniques of electrical engineering. The origins of this analysis can be traced to the works of Oliver Heaviside (1880's) and S. A. Schelkunoff (1) (1930's). It provides the means by which distributed circuits may be compared to, and analyzed as, lumped circuits and is a critical analytical link between lumped and distributed resonant systems. The usual presentation of the model is focused on the development of the impedance transforming properties of transmission line matching networks and does little to demonstrate or emphasize the resonant rise phenomenon. Figure 1 illustrates the it, $\lambda/4$ coaxial resonator as it would be represented in lumped equivalent circuit theory. As the analysis of distributed circuits represented in this form is extensive it will not be repeated here.

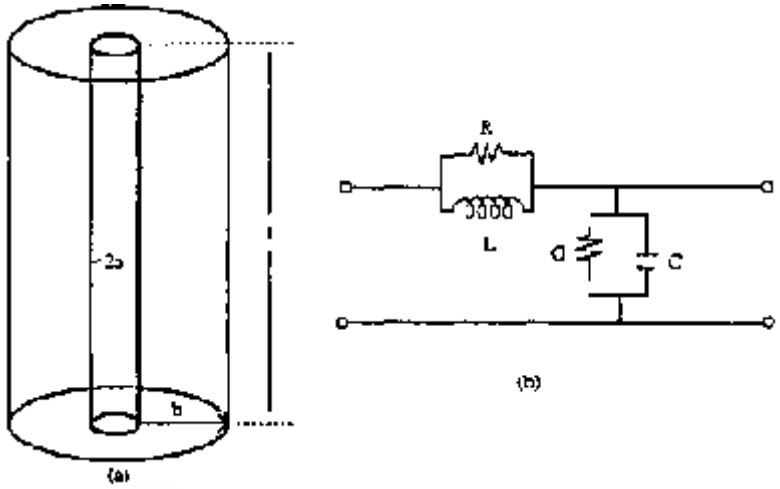

Figure 1(a): The $\lambda/4$ coaxial resonator - 1(b): The lumped equivalent circuit

The equations for the lumped equivalent parameters and the characteristic impedance are:

$$L = \frac{\mu}{2\pi}\ln(b/a)\,H/m \quad (1)$$

$$C = \frac{2\pi\varepsilon}{\ln(b/a)}\,F/m \quad (2)$$

$$R = \frac{R_S}{2\pi}\left(\frac{1}{a}+\frac{1}{b}\right)\frac{\Omega}{\pi};\; R_S = \sqrt{\frac{\pi f \mu_{cond}}{\sigma_{cond}}} \quad (3)$$

$$G = \frac{2\pi\sigma}{\ln(b/a)}\,S/m \quad (4)$$

$$Z_0 = 60\ln(b/a)\Omega$$

Resonance

The phenomenon of the resonant rise on a transmission line, and in any cavity resonator, is physically due to coherent reflection of forward and backward traveling waves occurring at critically spaced terminating surfaces. The occurrence of standing waves, or stationary field distributions, is common to all resonators and is indeed the mechanism by which energy storage and voltage, current and impedance transformation are realized in distributed circuits.

The simple field distributions of most cavity resonators share great qualitative, and indeed some analytic similarities with the standing waves present on transmission line resonators. A thorough conceptual appreciation of the phenomenon of resonant rise may be obtained from consideration of a vector diagram representation of the incident (E1) and reflected (E2) waves on a resonant length of line. Figure 2 shows the familiar sinusoidal voltage distribution associated with the open circuited lossless resonant line and the resulting phases of the two waves at different points in the distribution (2). Under lossless conditions the load reflection coefficient is unity with zero phase

angle and the load impedance is infinite. As a result, the incident and reflected waves have equal magnitudes at the load, and the reflection occurs such that the resulting phases of the two waves are also the same. As the figure demonstrates, this phenomenon yields a terminal point voltage that is the arithmetic sum of the incident and reflected components.

EL = $2E_1 = 2E_2$ (6)

It should also be noted that in this ideal case the currents of the incident and reflected wave are equal in magnitude but opposite in phase. Thus, the vector sum is zero and the current into the load is zero.

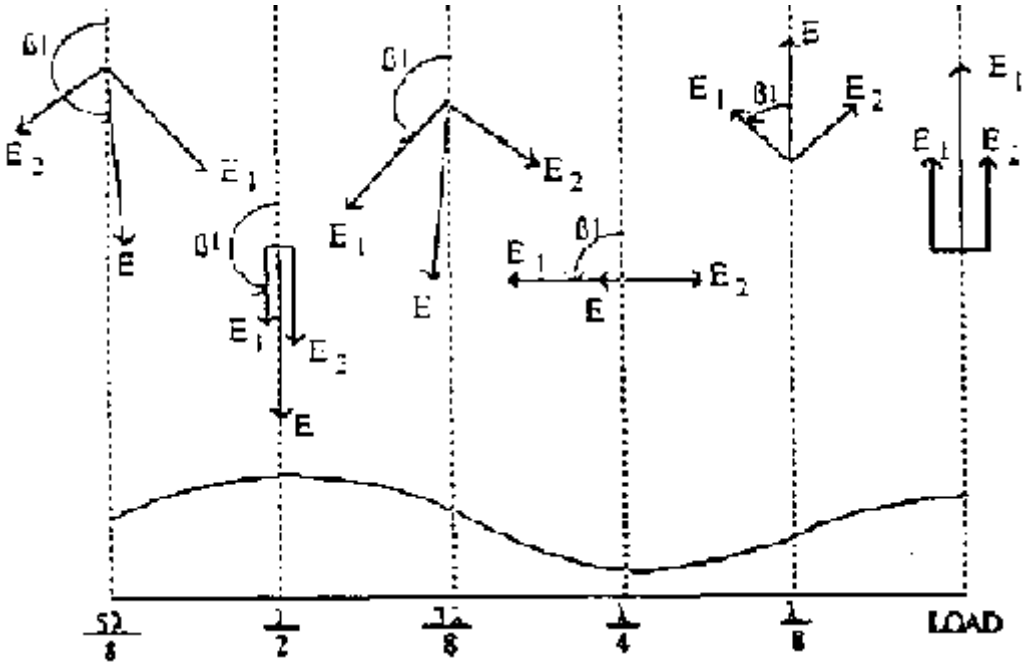

Figure 2. Vector Diagram representation of the incident and reflected voltage waveforms on resonant transmission lines (2)

The criteria for resonance is inherent in the spatial voltage distribution and requires the voltage maximum and minimum be separated by one quarter wavelength. This means that regardless of the loading, the system must be, electrically, ninety degrees long. This can be easily demonstrated with a Smith chart analysis of the capacitively loaded $\lambda/4$ resonator.

Foreshortened Coaxial Resonator

The example presented in this paper to illustrate the coaxial cavity resonator is a discharge device where the potential for discharge is built up in a spherical capacitor. It is appropriate to show how this capacitive load will change the operating parameters at the resonator. Numerical values presented are appropriate for the demonstration model. The material presented comes from published work (3) and is in part the result of mutual theoretical development conducted by the authors and Dr. F. Corum on this research project. (Some of this material will also be found in the monograph "Vacuum Tube Tesla Coils" by James F. Corum and Kenneth L. Corum).

For the capacitivly loaded transmission line, the length at resonance will be less than a quarter wavelength long due to the change in the angle of the reflection coefficient at the load end. The effect on the SWR is that the angle is reduced from 0 degrees, for a full $\lambda/4$ unloaded line, to a negative angle such that the reflection coefficient for the open-circuited end will be:

$\Gamma 2 - |\Gamma 2| / f$ where: f <0 (7)

The result of this change is that the line is not only physically shortened but that stationary >/4 sinusoidal field distribution is effectively shortened. Figure 3 shows the comparison between the unloaded and loaded distributions.

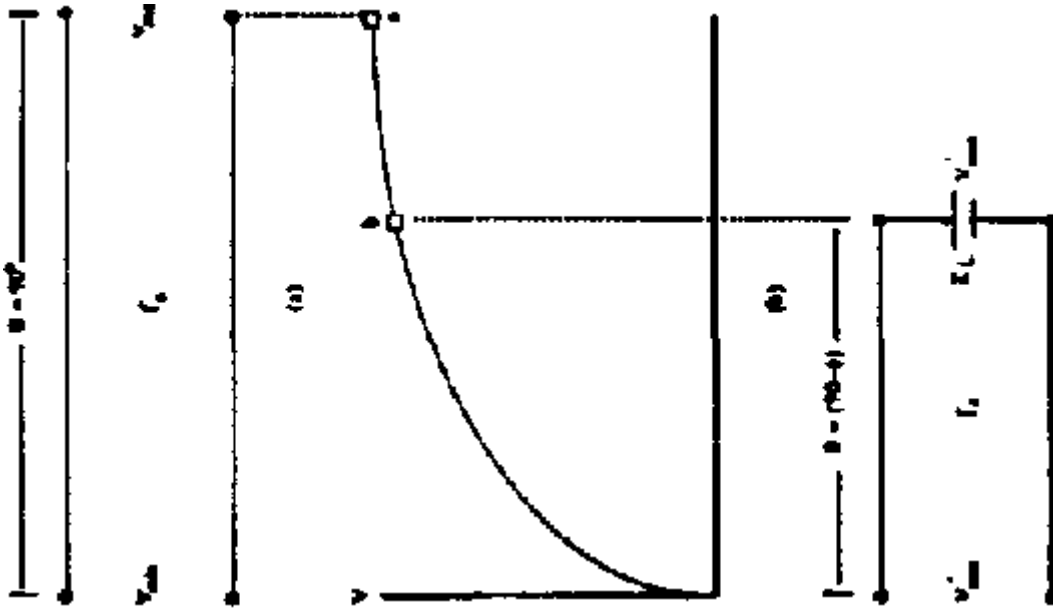

Figure 3. The capacitively foreshortened line: (a) unloaded line (b) voltage distribution (c) loaded line and resulting reduction in attained load voltage

Lumped Equivalent Example

Consider the resonator shown in Fig. 4 with its equivalent transmission line model. At the shorted input end (1) the impedance is (ZL = Rloss + j0) and the reflection coefficient ($\Gamma 1 = 0 < 180°$). At the load end (2) the capacitance of the sphere must be calculated and the load parameters evaluated.

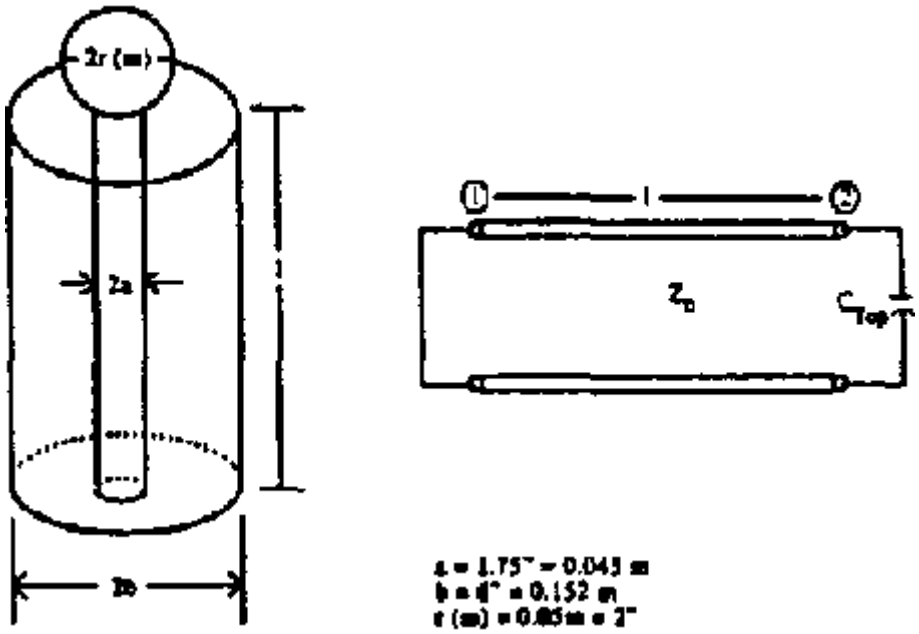

Figure 4. The capacitively top loaded coaxial cavity and its equivalent transmission line circuit for Smith chart analysis.

The capacitance to ground of an isolated sphere is given below and may be used as a reasonable approximation for the top loaded sphere.

C sphere = 4 pe o r (m) (8)

Where r(m) = radius in meters

Thus C top = 5.65 pF

The unloaded $\lambda/4$ resonant frequency of the line is calculated from:

$c = \lambda / 4 = 41$ (m)f, or f = c/ 41(m). (9)

This yields: f=100 Mhz, and $\omega = 2\pi f = 6.28 \times 10^8$ rad/sec.

Thus the proper load impedance is:

$$X_l = 1/j\omega C_{top} = 1/j\,2\pi f C_{top} = 281.7\Omega \quad (10)$$

The characteristic impedance of the resonator in an air dielectric is:

$$Z_0 = 60\ln(b/a) = 74.0\Omega \quad (11)$$

The normalized load reactance is:

$$X_l' = X_l / Z_0 = 3.81 \quad (12)$$

The effect of the loading capacitance is to require the line to be shortened to maintain the same resonant frequency or to lower the resonant frequency when added to a line of given length. The electrical line length with C top as a load will be:

I' (λ_0) = 0.25 λ_0 = 0.2875 λ_0 (13)

or

l'(m) = I' (λ_0) λ_0 (m) = 0.863 m

and the resulting resonant frequency is:

f' = C/4 I'(m) = 86.91 Mhz (14)

Coaxial Cavity Resonator

A transition from resonant transmission line to resonant cavity occurs for the coaxial line when the input is short circuited as shown in the Figure 5. Several things become apparent with this fundamental observation. The structure takes on the nature of a completely enclosed system, or hohlraum as they have been called (4), like that of a cavity is a traditional geometry exhibiting properties of both waveguides and cavities and is an important conceptual link for developing all classes of cavity resonators for application as RF power processing elements.

It may be shown that optimal dimensions of the coaxial cavities may be developed from criteria for maximizing the energy storage (Q) and step up (SWR) of the cavity. The criteria for development of maximum Q may be seen in the optimization of the Q from power considerations. The Q of a resonant cavity is defined as before:

$$Q = \frac{f_0}{2\Delta f} = \frac{(2\pi \text{ energy stored})}{(\text{energy dissipated per Cycle})} \quad (15)$$

The energy stored and dissipated is approximated as:

Energy stored = $\iiint \Phi^2 dv$ and Energy dissipated = $\iint \Phi ds$

Therefore:

$$Q \cong \frac{VOL}{A_s}$$

Thus, Q may be maximized for the geometry which yields the largest volume to surface area ratio. This occurs for the coaxial cavity when the ratio of (b/a) equals 3.6 and the resonator has a

characteristic impedance (Z_c) of 76.9 Ω (5). A comparison of obtainable unloaded Q's for different resonant systems is insightful. Table 1 shows the representative magnitudes of the various unloaded resonant circuits.

Table 1: Magnitudes of R sh for Resonant Structures

TYPE OF CIRCUIT	R_{SH} (MAGNITUDE) Ω
Lumped Tank	10,000
Tesla Coil	100,000
λ_4 Coaxial Resonators	100,000
Cavity Resonators,	1,000,000

.
The trend in increasing "Q" with increased volume to surface area may be seen progressing down the table. The coaxial cavity fares well comparatively with all structures and was chosen for the simplicity of construction and design as well as its representative nature. The Q's of cavity resonators exceed those of coaxial resonators by an order of magnitude and might be chosen as a superior system for certain applications of power processing.

The criteria for the development of maximum step-up (SWR) parallels the shunt resistance considerations since R sh - SWR.

$$R_{sh} = \frac{\left|\int V dl\right|^2}{P\,diss} \quad (17)$$

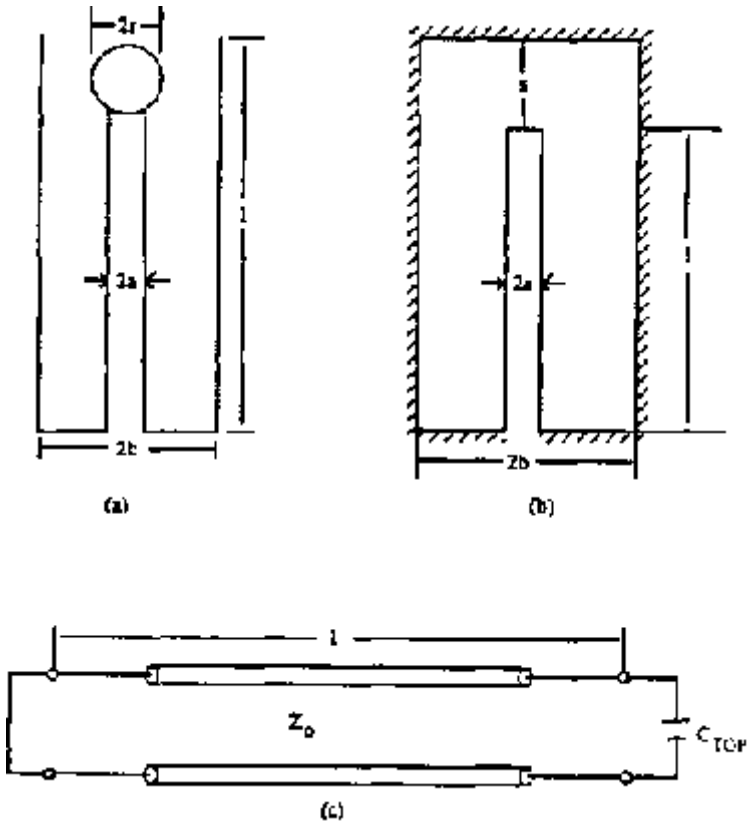

Figure 5. The quarter wavelength capacitively loaded cavity:

(a) spherical capacitively top-loaded cavity
(b) foreshortened capacitivly loaded cavity
(c) transmission line equivalent

It is obvious that the shunt resistance is a function of the conductor losses and loading. The maximum shunt resistance occurs for b/a = 9.2 which yields a characteristic impedance of 133.1 Ω (5).

Again, a comparison of obtainable shunt resistance (R sh) for different resonant systems is insightful. Table 2 shows the representative magnitudes of the various unloaded resonant circuits.

Table 2: Magnitudes of "Q_u" for Resonant Structures

TYPE OF CIRCUIT	Q_u (MAGNITUDE)
Lumped Tank	100
Tesla Coil	100
$\lambda/4$ Coaxial Resonators	1000
Cavity Resonators	100,000

RF Power Processing

The first individual in the literature to realize that the RF resonant systems might be used to advantage in the processing (or transformation) of large electrical energies for engineering applications was Nikola Tesla. He first developed the "distributed helical resonator" strictly as a means of generating high voltages and the resulting spectacular discharges for which he is famous. He completed extensive empirical testing and optimization of this structure during the late 1890's and proposed a variety of possible applications including wireless transmission of power and the concept of directed energy weapons.

When examining Tesla's Colorado Springs Device as a model for a power processing system four basic processes can be observed. The conversion of power from 60 Hz to RF; the transformation by pulse modulation to high peak power and variable duty factor; the input coupling system; and the output couple to the load, Figure 6. These block components may be implemented by standard RF techniques in a variety of ways depending on the magnitude of the powers to be processed and the desired efficiency. The blocks comprising the resonator have been developed in the preceding sections and only the source considerations remain to be considered. Tesla implemented pulse moderation via a special breakwheel. As the break occurs and the spark is quenched (Tesla used a magnetic field and forced-air to quench the spark quickly). The high voltage transformer reactance is reintroduced across the primary tank detuning it to lower the "Q pri" and reduce the impedance which is coupled into the secondary. The secondary, which is now free of the loading of the ringing primary, now rings at its self resonant frequency (f sec) which is identical to that of the extra coil where the voltage (V sec) is stepped by resonant rise (VSWR). The primary capacitance (C p) is recharged during the break interval.

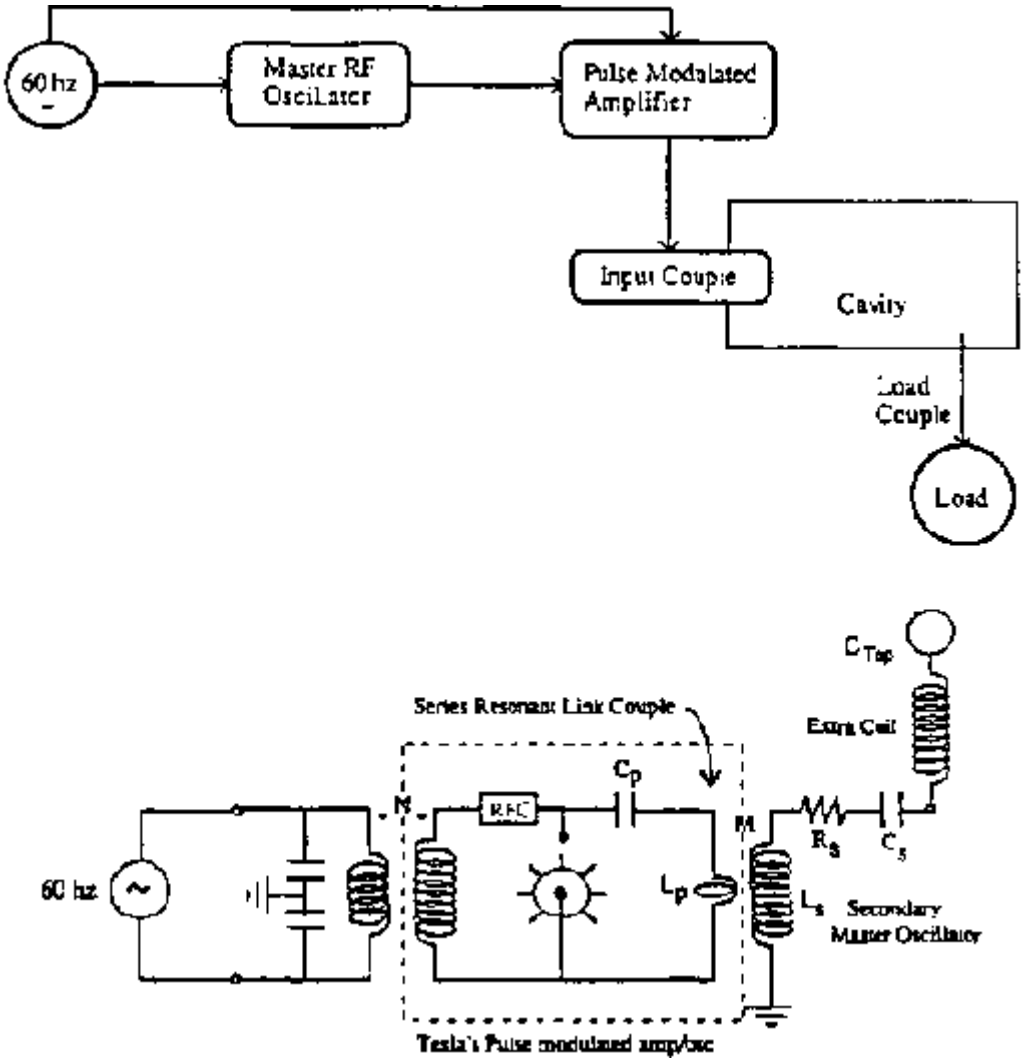

Figure 6: (a) Block diagram of typical RF power processing system (b) Tesla's 1899 Colorado Springs apparatus system equivalent. (3)

The spark interval during the exchange of energy between the primary and secondary must be carefully controlled to avoid reflection of energy back into the primary. For efficient operation, the optimal spark dwell must be used. This provides for trapping of the energy in the secondary/ extra

coil circuit which can be charged over many spark and break intervals to very large power levels. With repeated pulses of peak energy from the primary, the secondary master oscillator will charge the extra coil, and the system achieve base voltages which, when stepped by the extra coil, will exceed the breakdown potential of (C top). It should be noted that with the tight coupling used by Tesla in 1899 (k=0.6) practical for any of the resonator types, the breakwheel was required to switch with less than two cycles of oscillation i.e.:

$$\tau_{spark} = \frac{1}{100kHz} = 10\mu sec$$

This is a phenomenal achievement with a breakwheel switch or modulator. This became the fundamental limitation preventing Tesla from exploring higher frequencies and smaller resonator geometries. The advent of the vacuum tube switch (not the oscillator) would remove some of these limitations.

State-of-the-Art Switching

The appropriate engineering choice of a vacuum tube replacement for the breakwheel is the hydrogen thyatron switch. State-of-the-art tubes achieve rise times on the order of a few nanoseconds and fall times (deionization times) on the order of ten nanoseconds. If it is assumed that the pulse duration must be on the order of twice the fall time to provide an efficient waveform, it is obvious that attainable frequencies are no greater than 100 MHz. This may seem surprising considering the frequencies attainable by "Class C" oscillators (GHz). However, with the currently available dielectric insulators this is as high a frequency (due to the resulting physical sizes) at which the physical dimensions of any of the open or cavity resonators can hope to be effectively insulated for high power applications (hundreds of kilowatts).

A variety of power oscillators designs have been developed for different applications in industry and have become part of many standard texts on vacuum tube electronics. One in particular suggests the basis for the development of another alternative. In the tuned grid-tuned plate oscillator the grid circuit acts as a master oscillator to drive the parallel tank in the plate circuit. The plate tank is tuned to a slightly different frequency from the grid circuit to provide a capacitive impedance large enough such that the capacitance in combination with that from the grid to plate of the tube meets the Barkhausen criterion. The use of a master oscillator is one critical element advantageous for driving a resonator, the removal of the double tuned circuit from the plate is another. Both of these may be achieved with a modified form of the tuned grid-tuned plate oscillator.

The general arrangement of this power oscillator is shown in Figure 7. It is to be noted that the link is untuned and must be constructed such that the grid to plate capacitance does not bring it to resonance and develop parasitic oscillations. This configuration avoids the spectral line splitting and efficiency limitations of the double tuned plate circuit and allows tight coupling to be utilized for efficient energy transfer to the resonator.

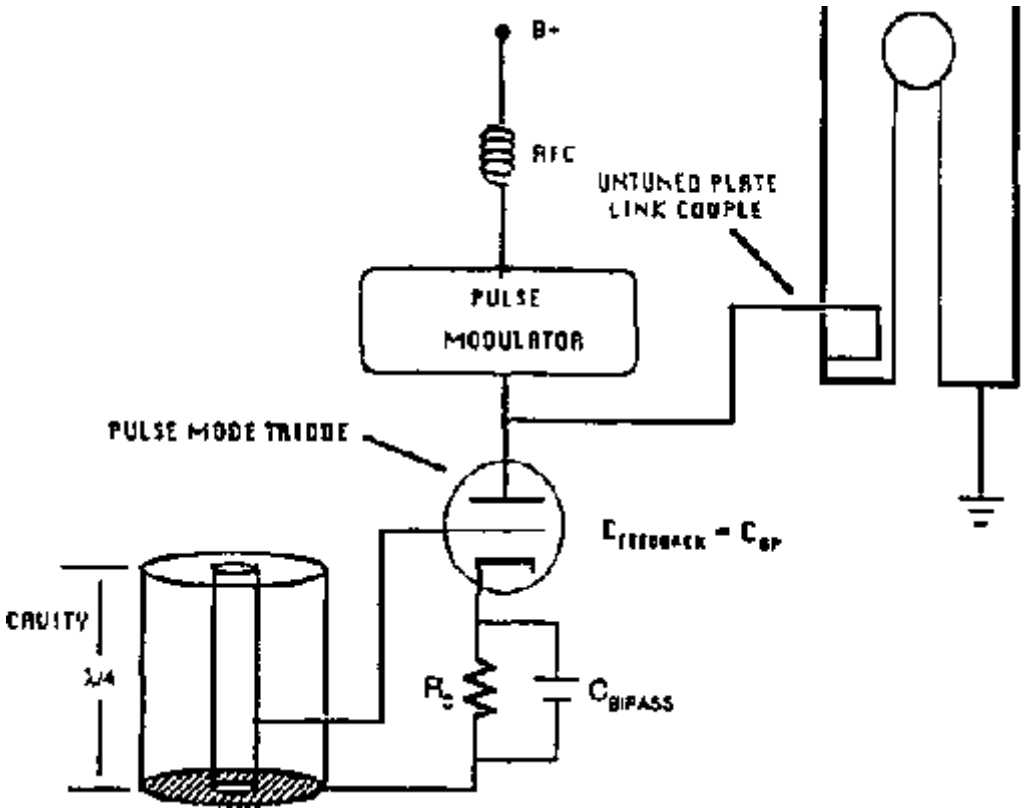

Figure 7: The optimal vacuum tube source configuration utilizing a tuned grid plate pulse modulated amplifier/oscillator with feedback via the grid to plate capacitance.

This is essentially a means of implementing an untuned plate circuit link coupled to the cavity resonator. The configuration places a master oscillator tank in the grid circuit so that the inefficiency of double tuned, coupled circuits is not present during the transfer of energy from the resonator to the high voltage discharge of the load. This is essentially a system paralleling the Colorado Springs Device and utilizing the insight provided by Sloan (6) in his work with early vacuum tube oscillators. The use of a distributed circuit (cavity) oscillator tank is advantageous in minimizing the tank circuit losses (principally the dielectric losses associated with gaseous dielectrics under pressure and the low losses characteristics of them. This characteristic bodes extremely well for the future application of resonant cavities to current high energy physics technologies.

Empirical Verification

Unfortunately the tubes needed to construct the device in Figure 7 do not exist or were not available. The capacitor discharge electrodes that were constructed were moderate in size and function well enough to give strong evidence of the potential for ~ /4 coaxial cavity resonators.

Two cavities were constructed and capacitively top loaded with small egg shaped (prolate spheroids) discharge electrodes as shown in Figure 8. The inner conductor length was chosen such that the electrodes partially protruded from the end of the outer conductor to provide for a compromise between minimization of the radiation resistance (cavity loading), the advantages of increased distance to the outer conductor (arc-over considerations), and the resulting visual display. Each of the geometries were empirically examined for agreement with the performance predicted by the analysis. And as the following analysis and results comparison shows, the empirical results of both were reasonable and fell within the expected magnitudes of performance.

As a result of a limited source power (= 200 watts C.W.) the magnitude of attainable voltage (= 20 KV) required the selection of very small spheroidal capacitor discharge electrodes. In fact any spherical capacitor designed to break down at approximately 20 kV has too low a capacitance to deliver any sizable charge to the spark discharge and to appreciably demonstrate lumped capacitive loading and foreshortening effects. The egg-shaped spheroid electrodes provide larger capacitance at a lower breakdown potential (though it is not accurately predictable). The concentration of

charge at the egg tip combined with the high E-field emission of charge for a small but impressively stable plasma discharge of two to four inches (5 to 10 cm) in length.

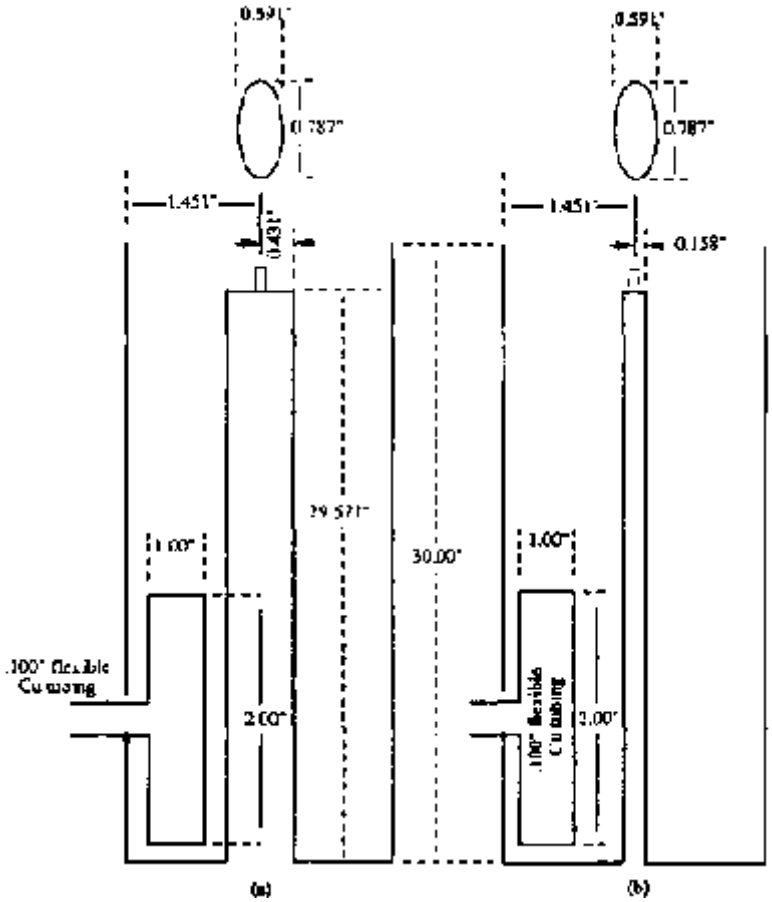

Figure 8: Experimental cavity dimensions (a) Cavity 1 b/a = 3.4; (b) Cavity 2 b/a = 9.2

The resonators were initially driven with a C.W. source (approximately 200 W) which yielded a vertical plasma (flame) two to three inches (5 to 7.5 cm) long which was fed or pumped by a bush type discharge approximately 1.0 to 1.5 inches (2.5 to 3.8 cm) in length. The source was then pulse modulated over a range of duty factors to allow the class A amplifier used to be driven at larger peak pulse powers while maintaining between 150 and 200 watts average power input.

This provided larger base voltages over pulse lengths sufficient to charge resonator to the breakdown potential of the discharge electrode. As a result of the larger base voltages obtained, the plasma length increased to between three and four inches (7.5 to 10 cm) fed by a brush type discharge 1.5 to 2.5 inches (3.8 - 6.3 cm) in length.

The brush type discharge is one of five types seen and characterized by Tesla in various experiments he conducted. As stated above, what was observed in this experiment was actually a I to 2.5 inch (2.5 - 6.3 cm) (this range in lengths covers the results obtained for both CW and pulse modulated sources) blue-white brush discharge occurring at rates sufficient to couple energy into and sustain a white RF plasma (two to four inches/five to ten cm long) producing temperatures at the base of the flame (not the hot centre) sufficient to melt the tip of an aluminum electrode (> 600 C). (Stainless steel was later introduced.) The larger discharges were achieved by pulse modulating the generator allowing the amplifier to be driven at higher powers for short pulse-periods (these being on the order of the fill time of the cavity). This produced higher peak voltages and hence the longer, hotter, and more stable discharges.

The discharges in the pulsed mode were driven with pulse repetition rates in the frequency range (100-10,000 pps). The modulation of the discharges at these frequencies produced an almost painfully loud audible frequency pitch. The frequency of the pitch was readily adjusted across the audio spectrum by varying the pulse repetition rate and the pitch was intensity was also seen to vary with changes in the pulse duration. This modulation, as well as the unmodulated excitation, was easily detected on FM radio receivers within a few hundred feet (approximately 100 m) due to

the intensity of the stray reactive fields off the end of the resonator. The radiated field components were measured at less than a milliwatt and are entirely negligible.

Coaxial Cavity Design Examples

The design of the coaxial cavity and the calculation of the parameters of interest for evaluating its performance, is directly obtained from analysis. The case of interest for evaluating the potential resonator performance and comparison to the empirical results is for the capacitively top loaded resonator with minimum loading presented by the input. coupling since this load can be effectively removed from the system by utilizing synchronous switching of the energy input.

The design parameters needed are:

a	=inner conductor radius (O.D)
b	= outer conductor radius (I.D)
la	= inner conductor length
or	(specify one or the other)
f	= desired frequency (MHz)
lb	= outer conductor length (if lb $\neq$ la)
Ctop	= top loading capacitance
ε_r	= relative dielectric permitivity

All dimensions will be worked in inches and frequencies in MHz unless otherwise specified. A reasonable estimate of Ctop is the first requirement. The top loading capacitance may be a spheroid or the foreshortening capacitance from the end of the inner conductor (terminated in a circular plate) to the outer conductor walls. Measurement of the cavity frequency responses were done with the spheroid discharge electrode removed and therefore with Ctop equal to the foreshortening capacitance. The recorded discharge parameters were obviously obtained with the spheroidal electrodes as the top loading capacitance.

The foreshortening capacitance may be roughly estimated from the area of the outer cylinder which extends beyond the inner conductor.

$$C_{top}^{fs.} = \frac{\varepsilon_0 A}{d} \quad (18)$$

Where:

A = π 2b(lb - la) = (area of the end of outer conductor)

d = b - a/2 = (mean distance to outer conductor)

The capacitance of the spheroid electrode used may be evaluated from an estimate of the mean diameter approximated by a cylinder of the same surface area.

$$C_{top}^{s.c.} = 4\pi\varepsilon_{r\,mean}(m) \quad (19)$$

This equation is for an isolated elevated sphere above a ground plane and does not account for the increased capacitance due to the vicinity of the surrounding outer conductor. For a rough approximation the value for the elevated body above a ground plane can be increased such that:

$$C_{top}^{i.e} = 1.5(C_{top}^{s.c.} \text{ over ground plane} \quad (20)$$

For small capacitance loads (Ctop << C) (i.e. when the top loading capacitance is less than ten percent of the resonator capacitance) a reasonable estimate of the foreshortened resonant frequency (fd) may be obtained as follows.

Determine the approximate frequency of operation (f_0) from the inner conductor strength.

$$f_a(Hz) = \frac{V_f c}{4l} \quad (21)$$

For linear conductors (fast wave structures) the velocity factor is assumed to be: Vf = 0. 999.

The load impedance is then calculated from the appropriate top loading capacitance.

$$Z_L = \frac{1}{j_\omega Ctop} \quad (22)$$

The characteristic impedance is:

$Z_0 = 60\ \mathrm{In}(b/a)$ (23)

The load reflection coefficient is then calculated from these values.

$$|\Gamma_2| \angle \phi = \frac{Z_L - Z_0}{Z_0 - Z_L} \quad (24)$$

The calculation of Γ_2 is unnecessary if there is no radiation resistance component included (i.e. Γ_2 = 1.0$<\phi^3$ for pure reactive loads) but is included here to demonstrate the effects of the loading resistance if it is not negligible (i.e. if large protruding discharge electrodes are used). At resonance:

$$\left[\phi - 2\beta\, la = -\pi\right] \text{ where: } \beta = 2\pi / \lambda_0 \quad (25)$$

Therefore, the approximate resonant wavelength is:

$$\lambda_0 - \frac{4\pi la}{\pi + \phi} \text{rad. or } -\frac{720^c la}{180^0 + \phi} \text{deg.} \quad (26)$$

The estimated resonant frequency (to within 2%) is then:

$$f_0 = \frac{V_f c}{V_f \lambda_0} \text{ or } f_0(Mhz) = \frac{11808.00(0.999)}{V_f \lambda_0 (in.)} \quad (27)$$

The electrical length of the resonator may be calculated from equation 28:

$$\theta = \beta_l = \frac{2\pi l}{V_t \lambda_0} \text{rad.} \quad (28)$$

The attenuation factor (α) is calculated from equation 29:

$$\alpha = 6.9462 \times 10^{-7} \frac{\sqrt{f(\text{MHz})}\left[1 - \frac{b}{a}\right]}{2b \ln\left(\frac{b}{a}\right)} \text{Np / in.} \quad (29)$$

The propagation loss is (αl) and the Qu of the resonator can be calculated from equation 30.

$$Q = \frac{\pi}{4\alpha l}$$

The final parameter of interest before calculating the step-up is the base impedance (Rbase) calculated from equation 31.

$$\text{Rbase} = Z_0 \left[\frac{1 - e^{2\alpha l}}{1 + e^{-2\alpha l}}\right] \quad (31)$$

Rbase is the input impedance of the cavity that the source (generator) would have to drive (or be matched to) if the resonator were to be driven by direct connection at the base.

The step-up is then calculated from equation 32.

$$\frac{\text{Vtop}}{\text{Vbase}} = \text{step up} = \frac{\left(\left[1 + |\Gamma_2| \cos\Phi\right]^2 + \left[|\Gamma_2| \sin\Phi\right]^2\right)^{\frac{1}{2}}}{\left(\left[e^{\alpha_1} \cos\theta + |\Gamma_2| e^{-\alpha_1} \cos(\phi - \theta)\right]^2 + \left[e^{\alpha_1} \sin\theta + |\Gamma_2| e^{-\alpha_1} \sin(\phi - \theta)\right]^2\right)^{\frac{1}{2}}} \quad (32)$$

Consider the following examples:

Example 1: Maximum "Q" Design b/a = 3.4:

Let:

a =	0.431 in. (1.095 cm)
b =	1.451 in. (3.686 cm)
la =	29.577 in. (75.126 cm)
lb =	30.000 in. (76.200 cm)
ε_r =	1.0

Example 2: Maximum (Rsh) Design b/a = 9.2:

Let:

a =	0.158 in. (0.401 cm)
b =	1.451 in. (3.686 cm)
la =	29.577 in. (75.126 cm)
lb =	30.000 in. (76.200 cm)
ε_r =	1.0

The results of these theoretical calculations are given in Table 3. It is to be noted that the results are from the estimated top loading capacitance and therefore are not strictly accurate. However, the estimates do agree well (within 1%) with operating frequencies measured in the lab and hence may be used with reasonable confidence.

Estimated Load C_{Top}	Z_o (Ohms)	Z_L (Ohms)	ϕ (Deg.)	Γ_o (Mag.)	θ (Deg.)	αl (Np)	Q_U	V_{Top}/V_{base}
Example 1 b/a = 3.8								
$C_{Top} = C_{DE}$ C_{Top} = 1.25pF	72.8	- j1273	- 6.55	96.08	86.81	2.47×10^{-4}	3180	664
$C_{Top} = C_{FS}$ C_{Top} = 0.7 pF		- j2274	- 3.67	97.68	88.26	2.52×10^{-4}	3120	596
Example 2 b/a = 9.2								
$C_{Top} = C_{DE}$ C_{Top} = 1.25pF	133.0	- j1273	- 11.93	93.10	84.12	3.14×10^{-4}	2500	656
$C_{Top} = C_{FS}$ C_{Top} = 0.7 pF		- j2274	- 6.69	96.01	86.75	3.19×10^{-4}	2460	591

Table 3. Tabulated theoretical results for critical parameters

The theoretical results are also obtainable, for the line without capacitive top loading, by calculating the lumped equivalent parameters and the equivalent equations to those above. This proves to be an appropriate method of calculation when coupling considerations and design are to be developed. The material constants of the cavity may also be changed from an air dielectric and copper conductor to any alternatives more easily than with the above method (the constants of the above equations include the material constants). A list of the material constants used is given below. The following calculations are done in meters to allow use of the more familiar constant values.

List of Material Constants

σ_{cu} =	5.65 x 10 mhos/m

μ_{cu} =	o = 1.257 x 10-6H/m
ε_r =	1.0
σ_{air} =	2.5 x 10- i 4 mhos/m

The propagation losses (αl) can now be calculated and the resulting Qu and the SWR determined from equations 33, 34.

$$SWR = \frac{1}{\alpha l} = \frac{8Z_0 f(Hz)}{RNc(m/s)} \quad (33)$$

The foreshortened SWR is then:

SWR' = SWR sin(90 - ϕ °) and

$$Qu = \frac{\pi f}{\alpha C} = \frac{2\pi f Z_0}{RC} \quad (34)$$

The results of the two examples are tabulated below for comparison.

Example 1: Maximum "Q" b/a = 3.6:

αl = 2.58 x 10^4 Nepers
Qu = 3,040
SWR = 3,880

Example 2: Maximum Rsh b/a = 9.7:

αl = 3.37 x 10^{-4} Nepers
Qu = 2,330
SWR = 2,970

Empirical Results:

The response curves of the two example cavities without capacitive top loading were measured in the lab with a link coupled input load on the cavity. The singly loaded "Q" of each was then calculated from plots of these curves shown in Figures 9 and 10. Though this is not directly comparable with the calculations of the unloaded "Q" above, it does place the magnitudes of the obtained results approaching the expected values.

f(MHz)	f_0(0dB)	f_L(-3dB)	$f_{u(}$-3dB)Q_L	
cavity 1	96.877	96.852	96.917	1938
cavity 2	95.640	95.611	95.690	1648

Table 4: Experimental Data for Determination of QL'

The loaded Q, (QL') was then calculated from equation 35:

$$Q = \frac{f_0}{2\Delta f_{L,U}} \quad (35)$$

The usual form of equation 35 in texts is:

$$Q = \frac{f_0}{\Delta f} \quad (36)$$

where; Δf is the difference in frequency found between the 3dB down points (Δf = fu - fL) of the response curve. The equation has been modified such that Δf is a measure of the difference in frequency between f_0 and the 3dB down points of the response curve (Δf = f_0 - fL) in this case.

This change was made to allow for the computation of the QL' such that the capacitive loading effects of the link couple, observable in the non-symmetric nature of the right half of the response curves (fo › › fu), did not effect the calculation and a closer approximation of the unloaded "Q" could be obtained (i.e. as close an approximation to the unloaded "Q" is desired). This loading is not a critical concern since it may be effectively removed by synchronous switching of the source energy. Thus, a reasonable approximation of the singly loaded Q (this is the "Q" with input coupling reduced to a minimum), QL', may be obtained from the equation:

$$Q_L' = \frac{f_0}{2\Delta f_L} \quad (37)$$

This is accomplished by minimizing the coupling (rotating the link such that it is parallel rather than perpendicular to the lines of magnetic flux) and measuring the response with a probe, achieving slight coupling to the reactive fields at the open end of the cavity as described above. The results obtained for QL' of each of the cavities are in Table 4 (and Figures 9,10) with the data needed to calculate them.

Empirical measurement of the step-up is prohibitive since any attempt to measure Vtop results in an additional capacitive load on the resonator and detunes it from resonance. A rough approximation of the potential can be made from the length of the brush discharge which is approximately:

$V_{\text{break down}}$ = 10 kv/in, = 10% (38)

The brush discharge was observable as a blue-white discharge beginning at the tip of the egg shaped discharge electrode as a typical arc, then forking or branching out at its end (over the final 30% of its length). It was most easily observed with a pair of welders goggles due to the surrounding white plasma (flame) which tended to wash out and mask the discharge outline. It is to be noted that all of the discharges occurred directly off the tip of discharge electrodes with vertical orientation, regardless of the orientation of the resonator (i.e. if the resonator was titled the discharge was maintained vertically).

The discharges were self initiating if the average power was of the magnitude of two hundred and fifty watts and the discharge electrode was clean. However, it could be started by placing a metal object such as a screwdriver tip near the tip of the electrode or passing a lit match across the tip with average powers on the order of 100 watts.

The brush discharges (not the plasma flames) of the respective cavities for the pulse modulated source were of the following dimensions, Table 5:

Table 5: Experimental values for determination of SWR'

Excitation	Device#	L_{dis}(in.)	L_{flame}(in.)	P_{avg}(Watts)

CW	cavity 1	1.0	2.0	200
CW	cavity 2	1.5	3.0	150
modulated	cavity 1	1.5	3.0	250
modulated	cavity 2	2.5	4.0	150

Example 1.

Ldis1 = 1.5 in. (3.8 cm)
Pavg = 250 W

Therefore; Vtop1 = 15.0 kv

Example 2:

Ldis2 = 2.5 in. (6.3 cm)
Vtop2 = 25.0 kv
Pavg = 150 W

The input voltage at the base of the resonator impressed by the generator may be estimated by:

$$Rbg = \frac{Z^2_0 \sin^2 \theta_1}{R} \quad (39)$$

From Figure 8, θ_1 (experimental) = 10°. So for cavity 1 with Z_0 = 72.8 Ω:

$$Rbg = \frac{(72.8)^2 \sin^2 10^0}{(50\Omega)} = 3.2\Omega \quad (40)$$

From Table 4:

$Vin_1 = | Rbg\ Pavg |^{1/2} = | (3.2)\ (250) |^{1/2} = 28.3$ Volts (41)

For cavity 2 with $Z_0 = 136.2\,\Omega$:

$$Rbg = \frac{(136.2)^2 \sin^2 10^0}{(50\Omega)} = 11.2\Omega \quad (42)$$

and:

$Vin_2 = |(11.2)(150)|^{1/2} = 40.9$ Volts (43)

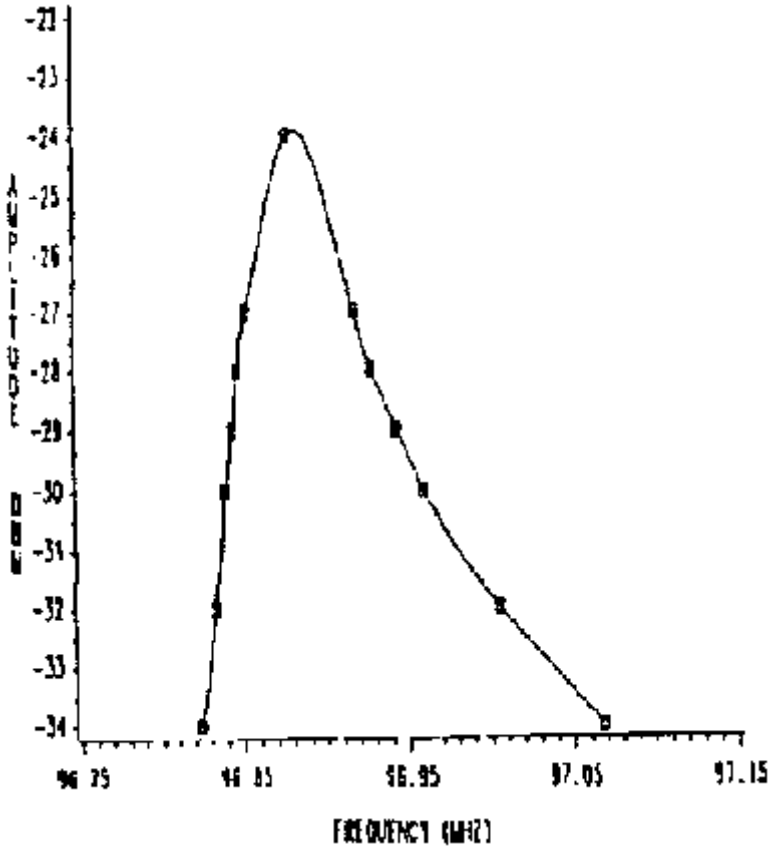

Figure 9. Response of cavity 1 (b/a = 3.4)

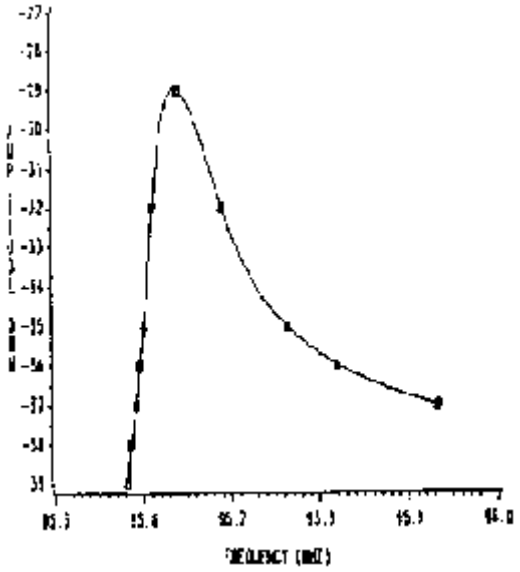

Figure 10. Response of cavity 2 (b/a = 9.2)

This yields the loaded step-up.

Example Cavity 1:

$$\text{step-up}_1 = \frac{15\text{kv}}{28.3\text{v}} = 530$$

Example Cavity 2:

$$\text{step-up}_2 = \frac{25\text{kv}}{40.9\text{v}} = 611$$

The step-up of cavity 2 should be approximately 25% higher than cavity 1 according to the analysis and as shown above, the experimental results fall within 10% of this predicted difference in the step-up.

Conclusions

The data did verify the ability to produce a discharge from the end of the inner conductor with relatively heavy loading on the cavity and unprecedented minimum power requirements with respect to the minimum power required to drive a Tesla coil to Ebreakdown with similar loading. Once started, either of the resonators were able to maintain the plasma of at least an inch with only fifty to sixty watts of input. Reduction in power input could be adjusted by reducing coupling or amplifier gain.

Recommendations have been made and commented on throughout the text to allow consideration of the topics as they are presented. The development of a full scale prototype RF power processing system is most definitely indicated to attain more accurate data as to the achievable efficiencies with state-of-the-art technologies. Additionally, a complete experimental determination of the loaded response of the cavity using pulsed excitation is necessary to evaluate the degree of efficiency obtainable with current technologies when using the phenomenon of switched resonant trapping. Such evaluation will allow targeting of new high power synchronous switch vacuum tube technologies for development.

Development of improved capacitive loads storing larger charge densities than uninsulated spherical discharge electrodes should be developed. The development of switches (controls) of high voltage discharges from such charge reservoir is feasible and should be investigated as a new high energy technology. This new application would provide means to accommodate the current directed energy technologies which might provide the needed impetus for further development of RF power processing technologies.

References

1. S.A. Schelkunoff. "The electromagnetic theory of coaxial transmission lines and cylindrical shields". Bell Systems Technical Journal. Vol. 4. p. 532-79. 1935.

2. F.E. Terman. Electronic and radio engineering. McGraw Hill. 1955. p. 91.

3. J.F. Corum and K.L. Corum. "A technical analysis of the extra coil resonator as a slow wave helical resonator", Proceedings, 2nd International Tesla Symposium. Colorado Springs p. 1-24. 1986.

4. W.W. Hansen. "A type of electrical resonator". Journal of Applied Physics. Vol.9. p. 654-63. Oct 1938.

5. T. Moreno. Microwave transmission design data. Dover. p.225-9. 1948.

6. D.H. Sloan. "A radio frequency high voltage generator". Physical Review. Vol. 47. p. 62-71. Jan., 1935.

LIST OF SYMBOLS

A =	magnetic vector potential
a =	(in.) inner conductors outer radius
b =	(in.) outer conductors inner radius
C =	(F/m) distributed equivalent capacitance

C_{Top} =	top (end) loading capacitance of resonator
C_{sphere} =	capacitance of an elevated metal sphere
c =	speed of light
d =	tap distance from shorted end of line
E =	electric field
f =	(Hz, MHz) frequency
f_0 =	circuit self resonant frequency
$f_{L,U}$ =	(Hz) lower and upper 3dB comer frequencies
G =	(Siemens/m) distributed equivalent shunt conductance
H =	magnetic field
i =	current
I =	current
K =	tapped x-mission line coupling constant
k =	coefficient of coupling
k_c =	critical coupling coefficient
L =	(H/m) distributed equivalent inductance
l =	l_a (in.) length of inner coax conductor
lb =	(in.) length of outer conductor if ($l_b \neq l_a$)

M =	mutual inductance coupling constant
N =	number of 114 wavelengths
Q =	resonant circuit quality factor
Q_{ul} =	unloaded Q
$Q_{l'}$ =	semi loaded Q (includes output end loading)
$Q_{l''}$ =	fully loaded Q (includes output end loading)
Q_{load} =	Q of the output (open end) load alone
r =	(m) radius of top loading spheroidal capacitance
R =	(Ω/m) distributed equivalent resistance
R_s =	skin effect resistance
R_o =	real portion of characteristic impedance
R_b =	resistance referred to the base of x-mission line
R_{bul} =	unloaded base equivalent transmission line resistance
S =	VSWR
T =	(sec.) phase period
T_{beat} =	(sec.) beat period of exchange of energy
t_{fill} =	(sec.) cavity resonator fill time
V_f =	velocity factor of a distributed circuit

v =	longitudinal phase velocity
X_L =	(Ω) load reactance of resonator (x-mission line)
Y =	(mhos)admittance
Z =	(Ω) impedance
Z_0 =	characteristic impedance of distributed circuit
Z_{in} =	impedance referred to the base of the line
$Z_{o.c.}$ =	impedance referred to open circuited end of line
$Z_{s.c.}$ =	impedance referred to shorted end of line
GREEK SYMBOLS	
α =	propagation attenuation constant
β =	propagation phase constant
Γ =	transmission line reflection coefficient
$\Gamma\|$ =	magnitude of reflection coefficient
γ =	($\alpha + j\beta$) longitudinal propagation constant
ε =	dielectric permitivity
ε_0 =	free space dielectric permitivity
η =	vacuum tube plate circuit efficiency
θ =	transmission line electrical length

λ =	wavelength
λ_0 =	free space wavelength
λ_g =	wavelength in propagating media and conductor
μ =	conductivity
ρ =	current density
σ =	conductance
τ =	pulse duration
τ_w =	cavity fill time rate constant
Φ =	magnetic flux
ϕ =	transmission line reflection coefficient phase
ω =	radian rotational frequency